INTERNATIONAL JOURNAL OF INTEGRATED ENGINEERING
ISSN: 2229-838X e-ISSN: 2600-7916

IJIE

Vol. 17 No. 5 (2025) 153-170
https://publisher.uthm.edu.my/ojs/index.php/ijie

The Effect of High-Performance Concrete on the Strength and Durability of Double Tee Beams

Sally Selan Hussein[1], Hussam Ali Mohammed[1], Ayad Ali Mohammed[1]*

[1] *Al-Furat Al-Awsat Technical University,*
Al-Mussaib Technical College, 51006, Babylon, IRAQ

*Corresponding Author: ayadia1@atu.edu.iq
DOI: https://doi.org/10.30880/ijie.2025.17.05.013

Article Info

Received: 4 August 2024
Accepted: 16 April 2025
Available online: 30 August 2025

Keywords

High-performance, precast double tee beam, prismatic section, compressive strength, durability

Abstract

This paper presented an experimental and analytical investigation of the behavior of a double tee beam under the influence of flexure by using High-performance concrete. Double tee beams can play an effective role in the span challenges in structural engineering by making a balance between material strength, geometric design, and load-carrying capacity. Three beams were tested experimentally with f'c equal to 30 MPa for the first beam and 40 MPa for the other two beams by making a model according to the available capabilities and testing it up to failure, the first beam was subjected to normal external conditions, and the other one was subjected to the effect of MgSO4 salt for six months. The result of the test show that high-performance concrete can save the strength of concrete as possible and protect the beam from corrosion. The difference ratio between the two tested beams equals 4.47%. Increasing the amount of compressive strength which is obtained as a result of using High-performance concrete had an effect in reducing the amount of stresses that occurred, thus reducing cracks and controlling their expansion. The beams were analyzed theoretically by using a powerful program (ABAQUS 2019) using the same mechanism of loading, same compressive strength, and material properties. The behavior of the beams is similar to their behavior from the experimental test with a difference ratio equal to (2.67% and 2.89%) for Double Tee Beam with the symbol DTB1 and DTB2, respectively.

1. Introduction

A double tee beam is a type of precast, prestressed concrete beam used in construction to support heavy loads over long spans. It is named for its cross-sectional shape. The double tee beam is a popular choice for construction projects that require large, open spaces without the need for intermediate support columns. The double tee beam is manufactured in precast concrete plants, where it is cast in a horizontal position using prestressing techniques. This involves tensioning steel strands or cables embedded within the concrete to enhance its strength and load-bearing capacity. The prestressing process helps to counteract the tensile forces that the beam will experience when subjected to loads. One of the key advantages of double tee beams is their high load-carrying capacity. The double tee shape provides excellent strength and stiffness, allowing the beams to support heavy loads over long spans. They are commonly used in parking structures, industrial buildings, bridges, and other applications where large, uninterrupted spaces are required [1].

In addition to their structural performance, double tee beams offer other benefits. They are manufactured off-site, which allows for better quality control and faster construction. The precast nature of the beams means that they can be quickly installed, reducing on-site construction time and minimizing disruptions to other

activities. Double tee beams also have excellent fire resistance properties due to the inherent characteristics of concrete. They are durable, resistant to weathering, and require minimal maintenance over their lifespan.

However, there are some considerations when using double-tee beams. Due to their size and weight, careful planning and coordination are necessary for transportation and installation. Specialized lifting equipment is typically required, and site conditions must be suitable for the maneuvering and placement of these large components. High-performance concrete (HPC) plays a crucial role in enhancing the performance of structure and durability of double tee beams.

High-performance concrete (HPC) offers several advantages when used in the production of double tee beams. Firstly, it provides increased strength, as it has a higher compressive strength than conventional concrete. This enables double tee beams to support heavier loads and span longer distances without requiring additional reinforcement. Secondly, HPC enhances durability due to its excellent resistance to external factors such as freeze-thaw cycles, chemical attacks, and abrasion. This extends the service life of double tee beams, reducing maintenance and repair costs.

Another significant benefit of HPC is the reduction in beam depth while maintaining structural integrity. This leads to cost savings in materials and construction and offers greater flexibility in architectural design. Additionally, HPC contributes to enhanced crack control, as it has lower shrinkage and improved tensile strength compared to traditional concrete. This minimizes crack development, ensuring better long-term performance and reducing structural risks.

So, HPC improves workability, facilitating easier placement and compaction during manufacturing. This ensures that the concrete fully fills the intricate shapes and voids within the double tee beam mold, resulting in a uniform and consistent final product. It is essential to emphasize that the specific mix design and composition of HPC can vary depending on project requirements and local conditions. The use of admixtures, such as superplasticizers and mineral additives, can further enhance the performance and workability of HPC in double-tee beam production [2].

The study of concrete beams in Magnesium Sulfate (MgSO4) solution is important because it helps understand the chemical interactions between concrete and the solution on the properties of the material, especially durability and corrosion. When concrete is exposed to MgSO4 solution, chemical reactions may occur that lead to the degradation of the concrete, reducing its strength and load-bearing capacity. These studies contribute to improving the design of concrete beams and selecting materials suitable for harsh environmental conditions. Additionally, understanding the effects of MgSO4 solution helps in studying long-term durability and guiding preventive measures to protect concrete structures from rapid deterioration [3].

In this paper, model is made relative to the standard dimension and experimentally tested and to study the effect of high-performance concrete by subjecting another bean with the same properties to an external effect (water with MgSO4 sulfate) for six months. Theoretically, the ABAQUS 2019 program was used to theoretically analyze the concrete beam using the finite element theory.

2. Experimental Work

2.1 Material Used for HPC Mixes-Portland Cement, Fine Aggregate, Coarse Aggregate, Silica Fume, and Superplasticizer are Used for This Purpose

In this research, KARASTA Ordinary-Portland Cement was utilized. This cement conforms to the Iraqi standard IQS NO.5-1984 [4] and the international standard BS EN 197-1:2011 CEM II/A-L 42.5 R [5]. Cement is produced in the Kurdistan region of northern Iraq. The cement must be stored in a dry environment to prevent exposure to external conditions.

2.1.1 Fine Aggregate (Sand)

Natural sand from (the al-Ekhaider region) was used as fine aggregate. The grading of fine aggregate is shown in Table 1. Water was used to wash and clean the sand, and then it was spread out and left in the air to ensure that the aggregates are free as possible from silt or clay because it reduces the cement aggregate bond strength and increases the water demand, also to get saturated and dry surface state before using it.

Int. Journal of Integrated Engineering Vol. 17 No. 5 (2025) p. 153-170

Table 1 *Grading of sand*

Sieve size (mm)	Cumulative passing%	Limits of Iraqi specification No.45/1984 (Zone 2))
10	100	100
4.75	96	100-90
2.36	91	100-75
1.18	84	90-55
0.3	8	30-8
0.15	2	10-0
pan	0	

2.1.2 Coarse Aggregate (Gravel)

Crushed gravel used for normal, high-strength concrete and high-performance concrete. The maximum size of 14 mm. Before being used, gravel was washed to remove clay and salts and then stored to attain a Saturated Surface Dry (SSD) condition. The grading of coarse aggregate (crushed gravel) is listed in Table 2.

Table 2 *Grading of coarse aggregate (crushed gravel)*

Sieve size (mm)	Cumulative passing%	IQS 45-1984 limits Size (5 to 14)
20	100	100
14	98	90-100
10	78	50-85
5	7	0-10

2.1.3 Silica Fume

Silica fume is also known as micro silica, condensed silica fume, volatilized silica, or silica particles. According to (ACI 234R-96, 2000) [6] silica fume can define as an ultra-fine, non-crystalline particle. It is typically a grey substance that resembles Portland cement or certain fly ashes. The diameter of the particles ranges from 0.1 to 1 m. This size is one hundred times smaller than the particulate size of cement. It is capable of displaying both pozzolanic and cementitious properties. It is filling the cavities, thereby decreasing the concrete's porosity and permeability. In addition, it could generate secondary hydrate C-S-H to create a stronger bond between the cement paste and aggregates in the interfacial zone (ASTM C 1240/2015). To prevent exposure to moisture, silica particulate must be stored in a dry, protected environment.

2.1.4 Superplasticizers (Sika)

Utilizing Sika's third-generation polycarboxylate polymer technology, Sika -180 GS is a high-range water-reducing, retarding, slump-retaining, and hyper-plasticizing admixture for Concrete & Mortar [7]. Sika is a potent superplasticizer with multiple functions, including surface adsorption and separating cementitious binder particles sterically. These properties provide the following benefits as the low water content results in high density, great strength, and low permeability. The superior plasticizing effect enhances concrete flow, ease of placement, and compaction. Shrinkage during curing is reduced, and creep after hardening is minimized. Steel reinforcement does not corrode due to the absence of chloride. The rate of concrete carbonation slows down. There is no need for vibration, which eliminates noise pollution. Its long-term stability makes it suitable for summer conditions and ensures pumpability.

2.1.5 Water of Mixtures

Normal water available in the laboratory was used in the blending and curing of specimens, mixing water had a temperature at (25±6°C).

2.1.6 Steel Reinforcement

For beam specimens, deformed steel rods were used as flexural reinforcement. For the webs used bars with 10 mm, were used as flexural reinforcement. For the flange used a mesh of bar with 6 mm. Test results of steel reinforcement bars are given in Table 3 and conformed to (ASTM A615-05) [8].

Table 3 *Steel reinforcement test results*

Diameter of Bar (mm)	Actual Diameter (mm)	Fy (MPa)	Fu (MPa)	Elongation Ratio %
6	5.90	400	490	9.5
10	9.79	420	630	13.2

2.2 Gradation of Aggregates

A new gradation was made for each coarse aggregate and fine aggregate used in the concrete mixture used in casting the mini-steel mold, where the amount of sand and gravel was sifted using standard gradation sieves. As for the coarse aggregate, after converting the standard gradient used in the normal mixture, which is 5-19 mm [9], and multiplying these dimensions by the reduction factor, we obtained a new gradient in which the size of the gravel was smaller than 9.5 mm.

As for the fine aggregate, the passing amount was taken through a sieve measuring 1.18 mm. Then a standard mixture was made by mixing both fine and coarse-graded aggregates with the amount of cement and water obtained from the method of designing standard concrete mixtures.

2.3 Concrete Mix

An optimal mixture design and carefully chosen high-quality ingredients are used to create high-performance concretes, which are then batched, mixed, put, compacted, and properly cured in accordance with the highest industry requirements. These concretes typically have a low water-to-cement ratio of 0.20 to 0.45. In order to make this concrete fluid and workable, plasticizers are typically employed.

Almost often, high-performance concrete is stronger than regular concrete. Strength, however, is not usually the most important requirement. High-performance properties would include, for instance, regular-strength concrete with extremely high durability and very low permeability. HPC has specified compressive strengths for the design of 35 MPa or greater (ACI 363R-92) [10]. It was consisting of (cement, silica fume, fine aggregate (sand), crushed coarse aggregate water, and superplasticizer (Sp). Table 4 shows the quantity of materials used in HPC mixesIllustrations

Table 4 *Materials quantity used in NSC and HPC*

	Cement kg/m3	Silica fume kg/m3	Sand kg/m3	Gravel kg/m3	w/c ratio	Water Content kg/m3	Super-plasticizer (by wt. of cementitious) %
	per m^3 of concrete						
NSC	367	---	704	1130	0.45	166	--
HPC	391	54	607	1042	0.37	145	2%

2.4 Casting and Curing

Plastic cubes were used to study the mechanical properties of each one. The molds were cleaned and oiled to prevent adhesion between concrete and molds. The fresh concrete should be placed in layers for the cube, each layer compacted by hand by using a compacted stick to reduce air voids After finishing the casting process, level the surface by using a steel trowel and left for 24 hrs in the laboratory. After 24 hours, it was removed from the mold and cured for 28 days by using burlap.

Another type of water used for studying the effect of external conditions is salt water. The use of this water is necessary to know the extent to which the concrete is affected by the salts in the water and the extent of the effectiveness of the used high-performance concrete.

Magnesium salts are the most effective on concrete when the concrete is treated with water containing the proportions of these salts. These salts were added to the water at a concentration of 6%, as this percentage is the most effective on concrete [11]. These salts interact with the cement paste and cause an increase in volume, which leads to the occurrence of cracks and corrosion in the concrete, especially in the edges and corners, as these sulfates cause tensile stresses in the cement paste, which affects its resistance.

Int. Journal of Integrated Engineering Vol. 17 No. 5 (2025) p. 153-170

Standard normal concrete cubes with a compressive strength of 30 Mpa were made, immersed in this water which contain MgSO4 after the period of curing, and tested after 120 days to compare it with other cubes immersed in normal water for the same period. Where a negative effect of these salts on the resistance was observed, as the standard cubes recorded a resistance of 31.87 MPa, while the cubes immersed in sulfate-containing water recorded a resistance of 24.6 MPa, with a decrease in compression by 22.81%.
And with the same mechanism, concrete cubes were made for a high-performance mixture with a resistance of 40 MPa, and they were also immersed for 120 days in normal water and another in water containing sulfate salts.

We notice through the results of the test that the intensity of the effect of these salts on the resistance was less for the cubes made of high-performance concrete. The standard cubes recorded a resistance of 41.2 MPa, while the cubes immersed in water containing salts recorded a resistance of 39 MPa with a decrease in compression by 5.34 %.

2.5 Prepare Beam Mold

The mold was made of steel with specific dimensions for the double tee beam relative to the standard dimension of beams used for construction by multiplying the real dimensions of the beam with a reduction factor equal to 1:7. The dimension of the mold and its shape is shown in Table 5 and Fig. 1, respectively. Fig. 2 shows the dimension of the stranded beam with a span equal to 18 m.

Table 5 *Dimension of the mold*

mold	Span length	Depth of beam	Width of double tee	Thickness of web (bottom)	Thickness of web (top)
Dimension (mm)	2500	140	330	20	30

Fig. 1 *Double tee mold*

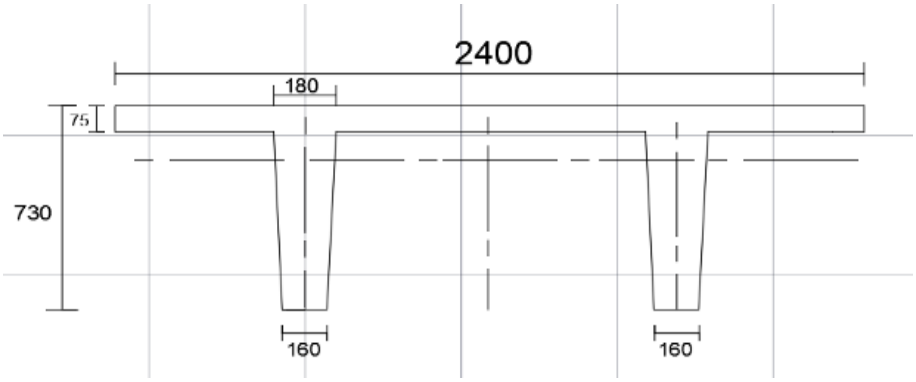

Fig. 2 *Dimension of standard beam*

2.5.1 Casting and Lubrication of Mold

Concrete components (coarse aggregate, sand, cement, and water), silica fume, and plasticizer were mixed in the case of high-strength and high-performance mixtures by using a mechanical mixer and mixing for 5 minutes. Then the molds are poured, taking into account the use of vibrators to ensure the homogeneity of the concrete components to obtain polished concrete and also to ensure the penetration of the concrete mixture with the reinforcing steel as shown in Fig. 3. For curing cover the surfaces of the beams with wet burlap. Each piece is removed from mold after 7 days. Ordinary grease is used to lubricate the mold to prevent the adhesion of the concrete mixture to the mold.

Fig. 3 *Casting of mold*

2.6 Laboratory Test

After curing the pieces of the double tee beam, the samples were collected for testing in the Structural Materials Laboratory. Before the testing, the samples were painted white after being cleaned to remove any dust or other debris from the surface. A hydraulic plate was applied to the samples in two load points 800 mm apart from the support, as shown in Fig. 4, and the load was applied gradually. The test method included just one system, which is a simple support. The length of the slab was 2500 mm, and the distance between the supports was 2400 mm. The load applied was a two-point load. The load was applied on the top of the beam and gradually increased by

Int. Journal of Integrated Engineering Vol. 17 No. 5 (2025) p. 153-170

the rate of 1KN. At each loading stage, the deflection is measured at midspan as shown in Fig. 4. The experimental test includes a load-deflection curve and ultimate load analysis.

Two beams were tested and symbolled by that:

DTB1: Double tee beam with f'c = 30 MPa.
DTB2: Double tee beam with f'c = 40 MPa subjected to normal conditions for six months.
DTB2: Double tee beam with f'c = 40 MPa subjected to the effect of MgSO4 salt for six months.

(a)

(b)

(c)

Fig. 4 *(a) DTB1 underloading; (b) DTB2 underloading; (c) DTB3 underloading*

2.7 Result of Experimental Work

2.7.1 Double Tee Beam 1 (DTB1)

This beam is tested up to failure. The support was made to achieve a simply supported state. The supports held the beam at a height of 22 cm. The compressive strength of this beam was 30 MPa. The deflection of the beam is measured at midspan. The load-deflection curve obtained from the test is shown in Fig. 5. The ultimate load is equivalent to 182 kN relative to the full scall dimension.

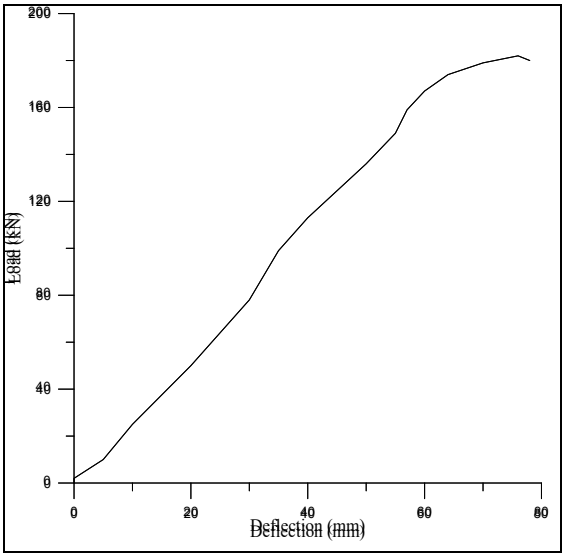

Fig. 5 *Load-Deflection curve for DTB1*

2.7.2 Double Tee Beam 2 (DTB2)

This beam is tested up to failure. The support was made to achieve a simply supported state. The supports held the beam at a height of 22 cm. The compressive strength of this beam was 40 MPa and it was subjected to normal external conditions for six months. The deflection of the beam is measured at the midspan. The load-deflection curve obtained from the test is shown in Fig. 6. The ultimate load is equivalent to 201 kN relative to the full scall dimension.

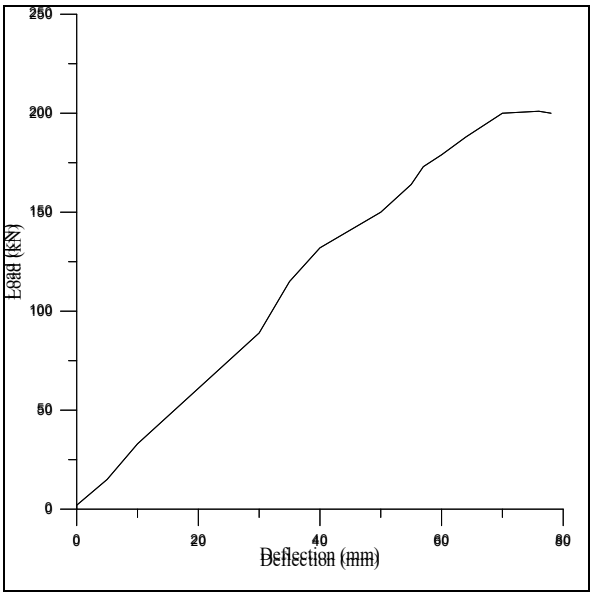

Fig. 6 *Load-Deflection curve for DTB2*

2.7.3 Double Tee Beam DTB2 with Long Term Effect

This beam is tested up to failure. The support was made to achieve a simply supported state. The supports held the beam at a height of 22 cm. The compressive strength of this beam was 40 MPa and it was subjected to the effect of MgSO4 salt for six months.

The deflection of the beam is measured at the midspan. The load-deflection curve obtained from the test is shown in Fig. 7. The ultimate load is equivalent to 192 kN relative to the full scall dimension. The difference in ultimate load between DTB2 and DTB3 is equal to 4.47%.

Int. Journal of Integrated Engineering Vol. 17 No. 5 (2025) p. 153-170

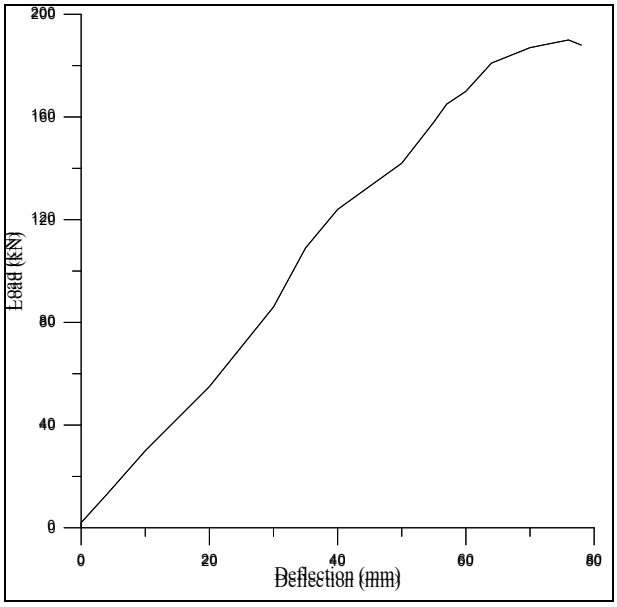

Fig. 7 *Load-Deflection curve for double tee beam DTB2 with long term effect*

3. Numerical Analysis

ABAQUS 2019 is a powerful program of engineering simulation depended on the finite element method that can solve problems spanning from relatively simplest linear analyses to the most difficult nonlinear simulations.

3.1 Modelling of Material

The ABAQUS program identifies two levels for each form of material: the elastic stage and the plastic stage. In the elastic stage, the elasticity modulus and passion ratio are determined. The type of material determines the type of plasticity employed during the plastic stage. Plasticity has been applied to the reinforced beams, while damaged plasticity has been applied to the concrete. CDP and elastic stage have only been used to characterize supporting and loading plates [12].

3.1.1 Concrete Description

The modulus of elasticity in the elastic stage is calculated using equations (1) (for normal concrete) and (2) (for high strength up to 83MPa) [13], as well as the poison's ratio of concrete between (0.15-0.22).

$$E_c = 4700\sqrt{f_c^{'}} \tag{1}$$

$$E_c = \frac{3320(f_c^{'})}{2} + 6900 \tag{2}$$

Five parameters in Concrete Damage Plasticity CDP should be represented by an ideal value for each type of concrete for the plasticity stage presented in Table 6 [14].

Table 6 *Plasticity parameters values used in ABAQUS*

Concrete type	ψ	ϵ	fb0/fc0	kc	Viscosity Parameters
NSC	34	0.1	1.16	0.667	0.0005
HPC	36	0.1	1.16	0.667	0.0003

3.1.2 Description of Reinforced Bar

In the elastic stage, the defined parameters were elasticity modules E and Poisson's ratio (υs) and they were used at the optimal value for a longitudinal bar with Ø10 mm and transverse bar of diameter 6 mm. While the second stage (the plastic stage) is represented by yield and ultimate stress with plastic strain, as indicated in Table 7.

Table 7 *The properties of bars used in the ABAQUS program*

Diameter mm	Elastic stage		Plastic stage			
	E Mpa	υs	Fy Mpa	Plastic strain	Fu Mpa	Plastic strain
Ø10	200000	0.3	420	0	630	0.074534
Ø6	200000	0.3	400	0	490	0.065443

3.1.3 Plate Description

The plate employed in support and boundary conditions, the materials defined simply by elastic stage, i.e., modulus of elasticity E and Poisson's ratio (υs) taken at optimal values of 200G Pa and 0.3.

3.2 Interaction Modeling

ABAQUS has interaction properties between distinct types of pieces after assembly for different regions of the sample

3.2.1 Coupling Interaction

At this stage, a reference point is established for applied loads within the bounds of a given loading region as shown in Fig. 8.

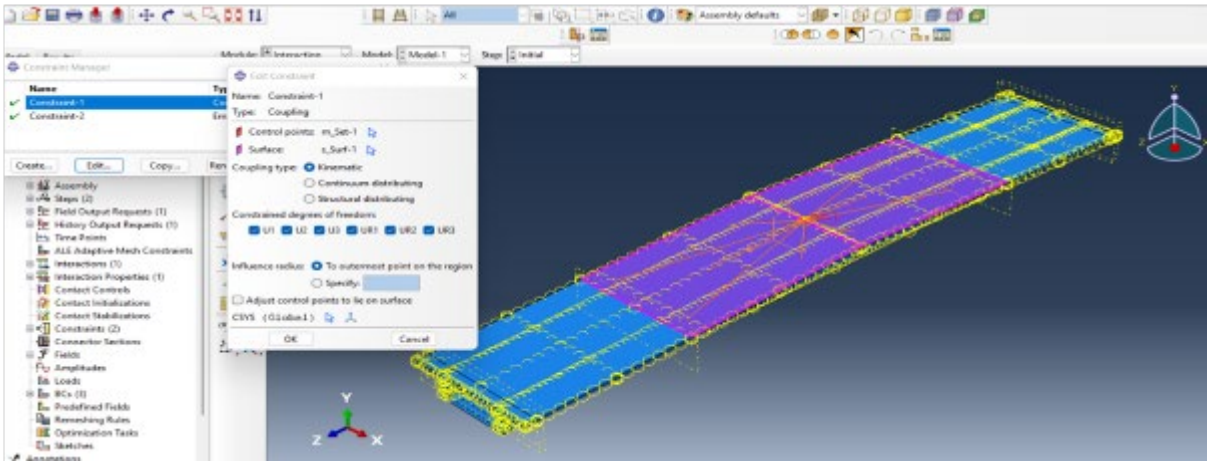

Fig. 8 *Interaction by coupling*

3.2.2 Embedded Region Interaction

In the "host" section of the model, which is where this form of constraint was applied, embedded elements or embedded groups of components were used. As a result, this method was used to embed reinforcement in the concrete "host" region. Because the degree of freedom for pore pressure and translational degree of freedom in nodes were eliminated, ABAQUS used the embedded node strategy from reinforcement with the closest node of the "host" region. This method is used when the reinforcement is entirely inside the concrete where the reinforcement elements are considered embedded within the concrete elements meaning that the displacement of the reinforcement fully follows the displacement of the concrete [15], as shown in Fig. 9.

Int. Journal of Integrated Engineering Vol. 17 No. 5 (2025) p. 153-170

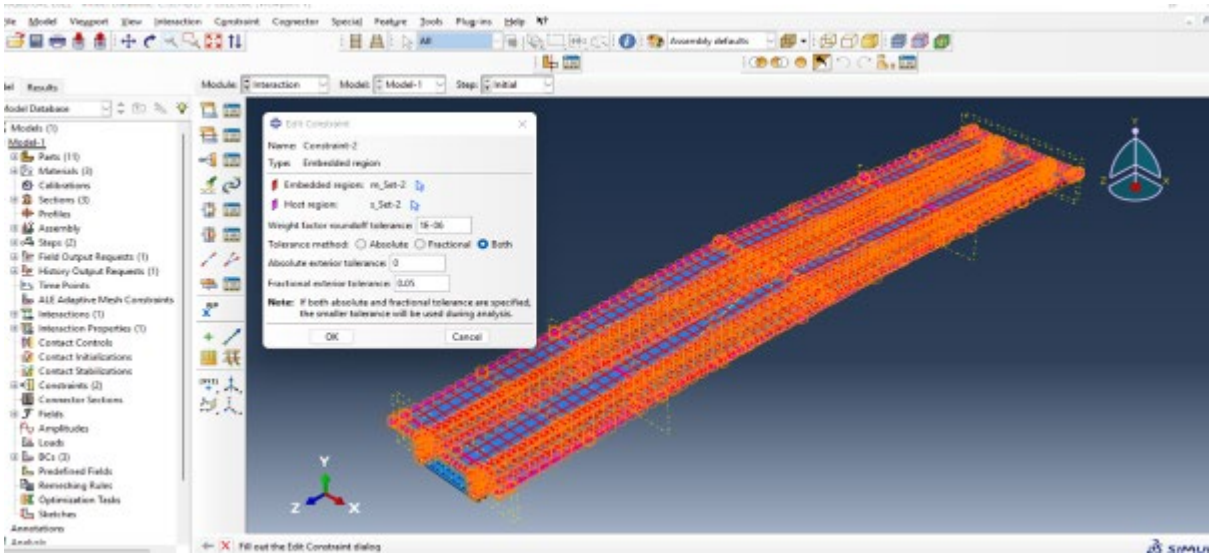

Fig. 9 *Interaction by embedded region*

3.2.3 Load Modeling

At this stage, a load is applied to the given area, depending on the type of load, whether it is distributed throughout the entire beam or in a specific area, or concentrated in specific places as shown in Fig. 10.

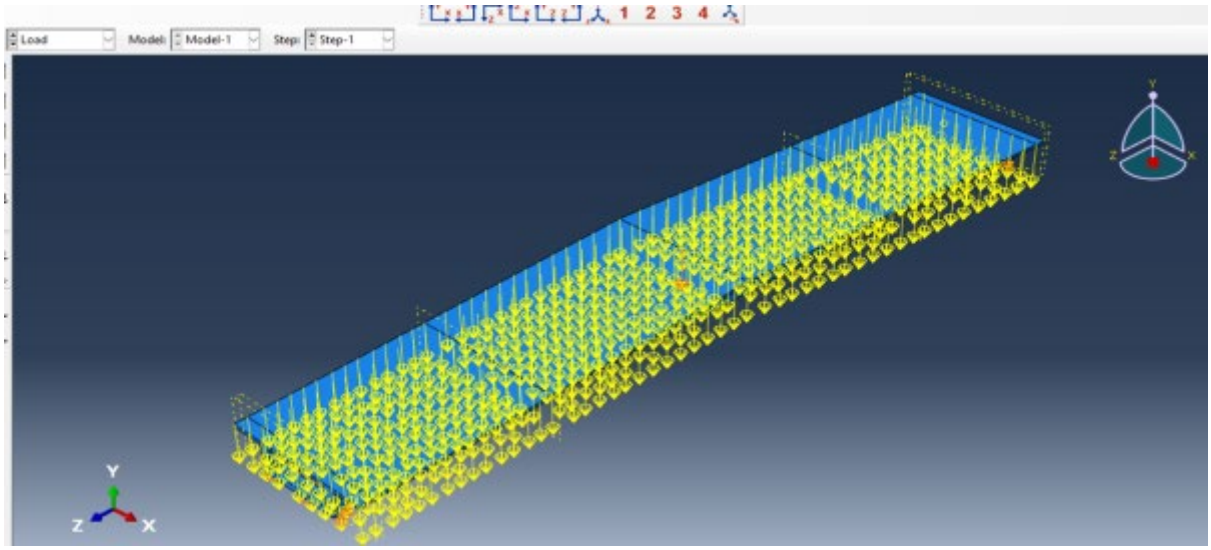

Fig. 10 *Modeling of load*

3.2.4 Surface-to-surface Contact Interaction

It must install the beam on the supports, and to prevent the stabilizers from separating from the beam, a connection is formed between them by making a tangential contact and assigning a penalty value of 0.4, as shown in Fig. 11.

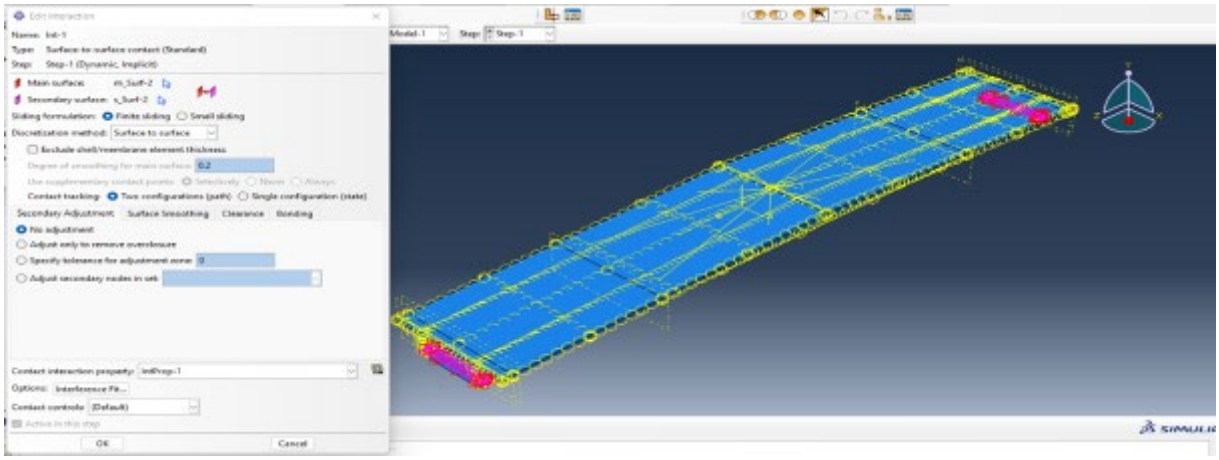

Fig. 11 *Interaction by making surface-to-surface contact*

3.2.5 Load Modeling and Boundary Conditions

The load was applied to the plate's node, and the boundary condition has been applied to the plate's surface. One of the supports was a hinged support (fixed in both the X and Y directions) and the other was a roller support (fixed exclusively in the Y direction). However, the load was applied to the node after the mesh for the plate was created, as shown in Fig. 12.

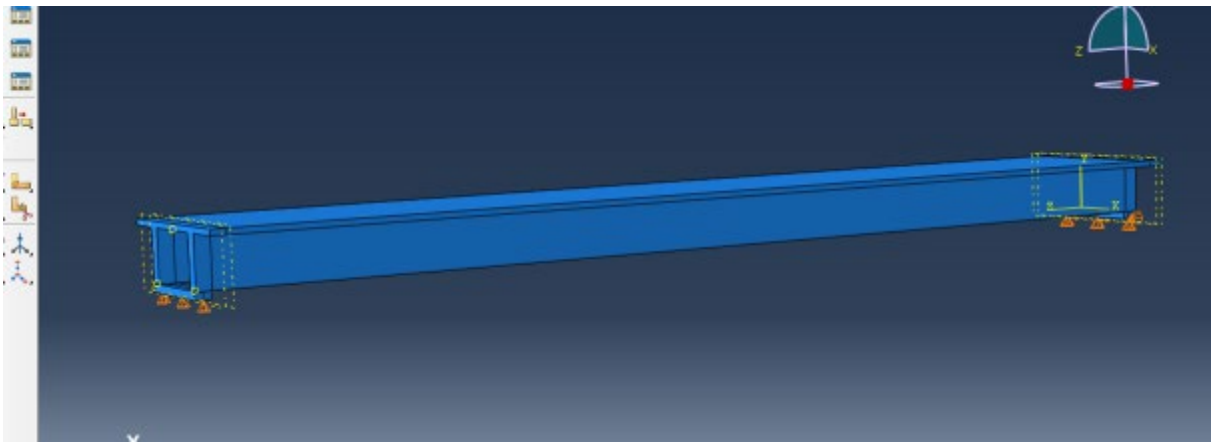

Fig. 12 *Modeling of boundary condition*

3.2.6 Beam Mesh

The beam is separated into small sections, and an approximate size value of 50 is assigned that is proportional to the length of the employed beam. The beam is then covered with a mesh that incorporates both concrete and reinforcement, with the possibility of modifying the type of reinforcement used, the truss instead of the beam. (Assign element type) which is brick element as shown in Fig. 13 [16].

Int. Journal of Integrated Engineering Vol. 17 No. 5 (2025) p. 153-170

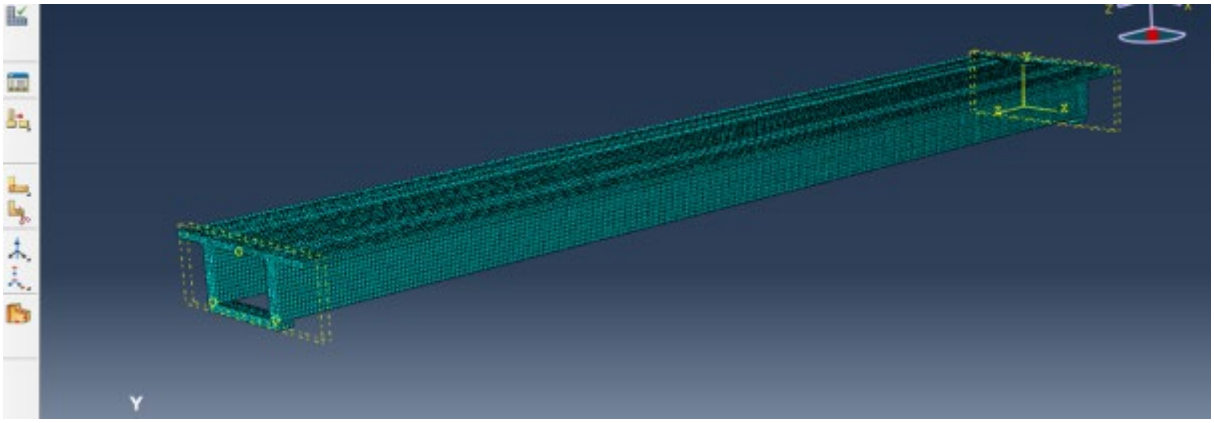

Fig. 13 *Mesh of beam*

3.3 Results of Numerical Analysis

3.3.1 Double Tee Beam 1 (DTB1)

In the numerical analysis used the same mechanism for loading, the same properties of the concrete section, and the compressive strength which equals 30 MPa. The curve was obtained from the numerical analysis and compared with the one from the experimental test. The results show good agreement between the two curves as shown in Fig. 14. The difference between the two curves obtained from the analysis was by the rate of 2.67%. This percentage was obtained by taking the average of all the points on the curve. Also, the variation of numerical longitudinal compressive strength along the flange width shown in Fig. 15.

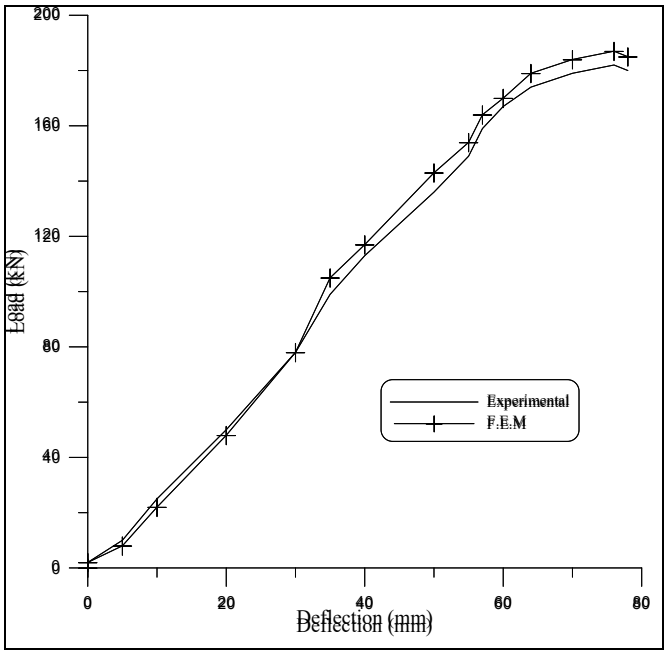

Fig. 14 *Load-Deflection curve for DTB1*

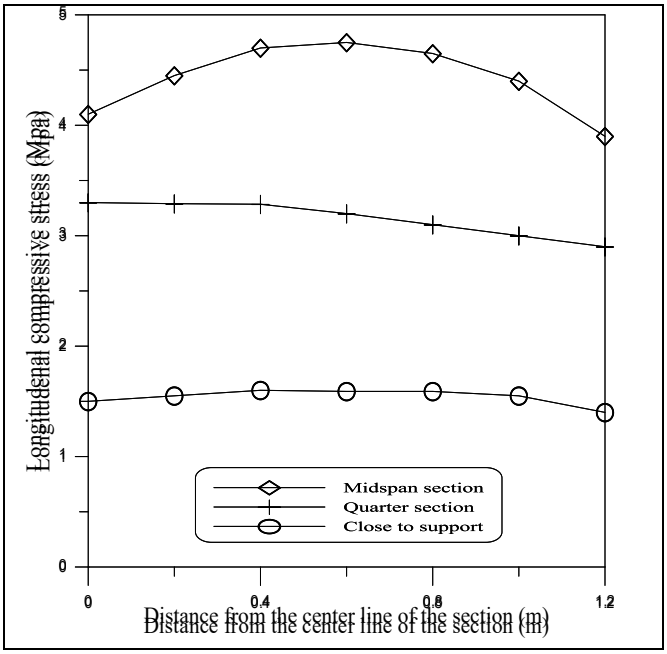

Fig. 15 *Distribution of numerical longitudinal compressive stresses along the flange width*

3.3.2 Double Tee Beam 2 (DTB2)

In the numerical analysis used the same mechanism for loading, the same properties of the concrete section, and the compressive strength which equals 40 MPa. The curve was obtained from the numerical analysis and compared with the one from the experimental test. The results show good agreement between the two curves as shown in Fig. 16. The difference between the two curves obtained from the analysis was by the rate of 2.89%. This percentage was obtained by taking the average of all the points on the curve. Also, the variation of numerical longitudinal compressive strength along the flange width shown in Fig. 17.

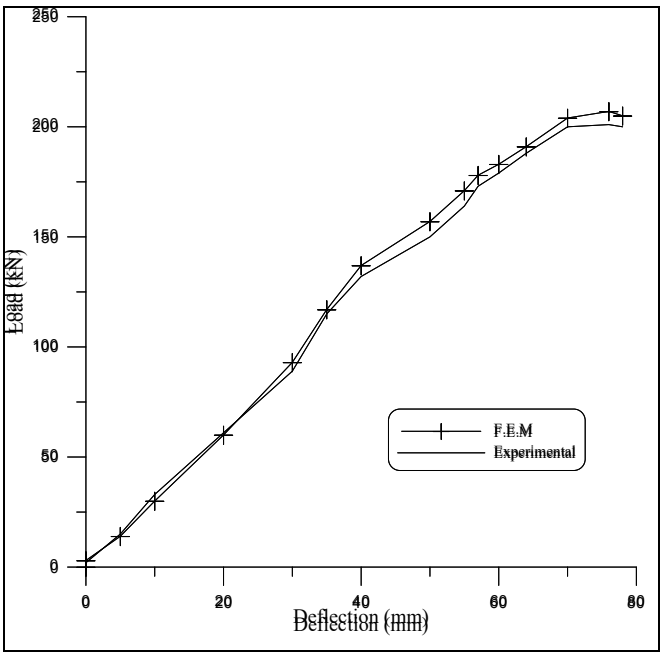

Fig. 16 *Load-Deflection curve for DTB2*

Int. Journal of Integrated Engineering Vol. 17 No. 5 (2025) p. 153-170

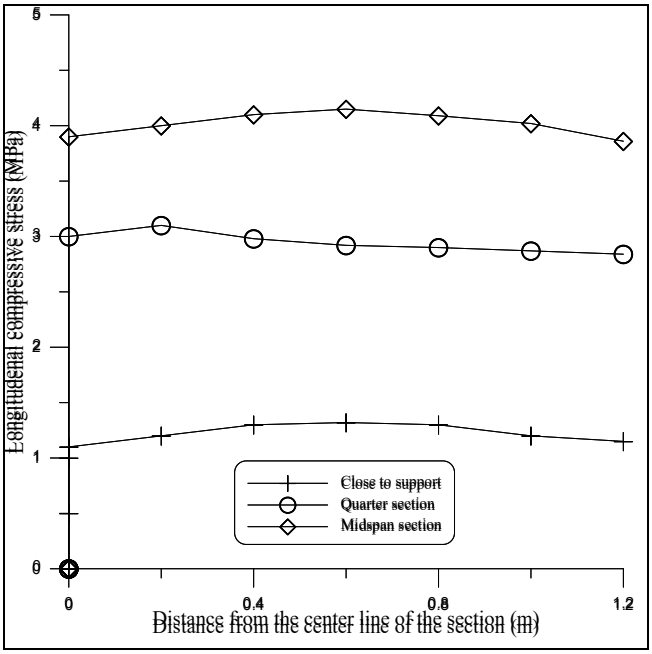

Fig. 17 *Distribution of numerical longitudinal compressive stresses along the flange width*

Stress reduction plays a significant role in reducing cracks in concrete beams. By managing the stresses within the beam, it is possible to minimize the occurrence and propagation of cracks. These stresses can be reduced according to many factors such as design consideration, adequate reinforcement, adding prestress, and properties of concrete, especially compressive strength. Herein the increase in compressive strength can reduce the stresses along the flange width of the beam as shown in Fig 15 and Fig. 17.

Fig. 18 *Places of appearance of crack causing failure (from experimental)*

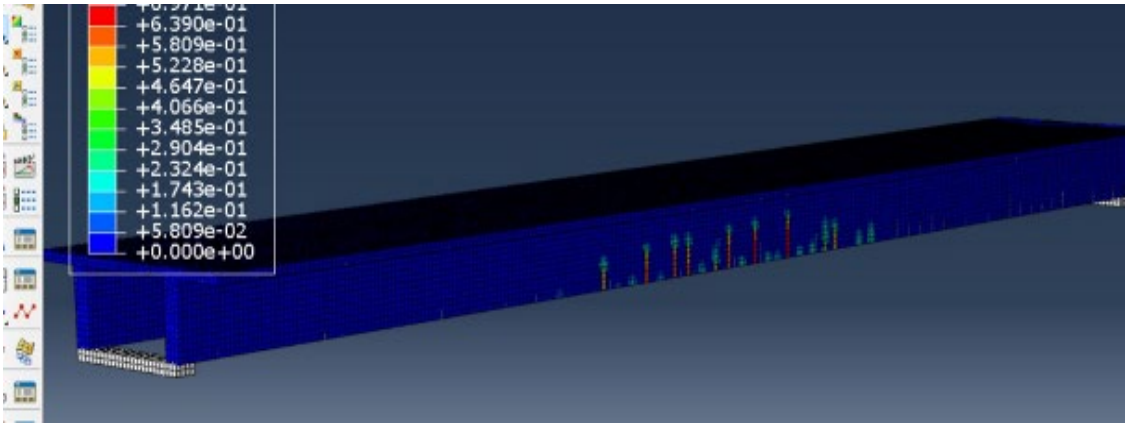

Fig. 19 *Places of appearance of crack causing failure (from analytical)*

The cracks occur in the prismatic beams when tested and are classified as vertical cracks at the bottom of the steam [17]. Where places of appearance of crack causing failure shown in Fig. 18 and Fig.19 for experimental and analytical, respectively. These cracks are usually predominant and more closely spaced in areas of greatest positive moment. This type of crack may occur according to Improper storage or handling of members, Bond failure at the end of and when the load began to exceed the load–carrying capacity of the member.

4. The Impact of Structural Parameters on Bridge Performance: A Comparative Study

Structural performance and durability are crucial factors in bridge engineering, influencing design choices and material selection. The research discussed in the conclusion examined the effects of high-performance concrete (HPC) on beam strength and durability. The experimental results demonstrated how HPC enhances structural integrity, especially under aggressive environmental conditions such as exposure to magnesium sulfate ($MgSO_4$). Studies by Naser et al. [18] and [19] provide additional insights into bridge performance by analyzing pier height effects and load rating evaluations. Their research on mathematical modeling of bridge piers highlights how structural components influence stress distribution and overall stability [18]. This aligns with the findings of the original research, which showed that material properties, such as concrete strength, directly affect structural resistance. Similarly, their flexure and shear load rating evaluation [19] emphasizes how different truck load types impact bridge superstructures, reinforcing the significance of analytical modeling approaches like the finite element analysis used in the study.

By integrating experimental testing with analytical modeling, both the original research and related studies highlight the importance of advanced material applications and structural assessments. The combination of high-performance materials and precise modeling techniques contributes to improved bridge durability and safer infrastructure development.

5. Conclusion

For the beams that are presented in this paper which were tested experimentally, the DTB1 is tested with f'c equal to 30 MPa under the effect of flexure, DTB2 is tested with f'c equal to 40 MPa with normal external conditions and DTB3 is tested with f'c equal to 40 MPa subjected to the effect of MgSO4 salt for six months. All beams tested up to failure. The ultimate loads are equal to 182 kN, 201 kN, and 192 kN for DTB1, DTB2, and DTB3, respectively. The effect of high-performance concrete was clear on the DTB3. The difference ratio between DTB2 and DTB3 equals 4.47%.

This percentage explains the effect of high-performance concrete by saving the strength as possible and protecting the beam from corrosion when compared with the effect of this type of salt on normal concrete so that the test improved the effect of using high-performance concrete by increasing the strength of beams and make them more durable.

Increasing the amount of compressive strength which is obtained as a result of using High-performance concrete had an effect in reducing the number of stresses that occurred, thus reducing cracks and controlling their expansion.

For the analytical analysis, the beams DTB1 and DTB2 are analyzed analytically by using ABAQUS 2019 using the theory of finite elements, and the results of the analysis are compared with the experimental test. The behavior of the beams is similar to their behavior from the experimental test with a difference ratio equal to 2.67% and 2.89% for DTB1 and DTB2 respectively. All percentage does not rely on a single value in the two curves but it was taken the average of these clear readings.

Acknowledgement

We would like to acknowledge the support given by the Al-Furat Al-Awsat Technical University, Al-Mussaib Technical College towards this project. We also thank our colleagues and collaborators for their support and assistance throughout the research process.

Conflict of Interest

The authors declare that there is no conflict of interest regarding the publication of this paper.

Author Contribution

The authors confirm contribution to the paper as follows: ***study conception and design****: Sally Selan Hussein, Hussam Ali Mohammed;* ***data collection****: Hussam Ali Mohammed, Ayad Ali Mohammed;* ***analysis and interpretation of results****: Sally Selan Hussein, Hussam Ali Mohammed, Ayad Ali Mohammed;* ***draft manuscript preparation****: Hussam Ali Mohammed, Ayad Ali Mohammed. All authors reviewed the results and approved the final version of the manuscript.*

References

[1] Nasser, G. D., Tadros, M., Sevenker, A., & Nasser, D. (2015) The legacy and future of an American icon: The precast, prestressed concrete double tee, *PCI Journal*, *60(4)*, 49–68, https://doi.org/10.15554/pcij.07012015.49.68

[2] Aïtcin, P. C., & Neville, A. M. (2007) High-performance concrete demystified, *Concrete International*, *15(1)*, 21–26.

[3] Zeng, X., & Yu, H. (2020) Review of studies on structural performance of basic magnesium sulfate cement concrete in China (2014–2019), *KSCE Journal of Civil Engineering*, *24(5)*, 1524–1530, https://doi.org/10.1007/s12205-020-0647-4

[4] Zena Abbas, A. K. (n.d.). Concrete technology second class: Manufacture of Portland cement.

[5] COMESA and SADC Harmonized. (2018) Cement – Part 1: Composition, specifications and conformity criteria for common cement.

[6] ACI Committee 234. (2006) Guide for the use of silica fume in concrete (ACI 234R-06, Reapproved).

[7] Sika. (2021) Sika® ViscoCrete® -180 GS product data sheet.

[8] American Association of State Highway and Transportation Officials. (2012) Standard specification for deformed and plain carbon-steel bars for concrete reinforcement (A615).

[9] Singh, K. (2016) Gradation of coarse aggregate by sieve analysis. Civil Engineering Portal. Retrieved from https://www.engineeringcivil.com/gradation-of-coarse-aggregate-by-sieve-analysis.html, 2016

[10] ACI Committee 363. (1992). State-of-the-art report on high-strength concrete (ACI 363R-92).

[11] Khaled Hassan. (2014) Effect of external sulfur attack on concrete, *Babylon University Journal/Engineering Sciences*, 22*(3)*, 581-593, https://search.emarefa.net/detail/BIM-441532

[12] Hafezolghorani, M., Hejazi, F., Vaghei, R., Jaafar, M. S. B., & Karimzade, K. (2017) Simplified damage plasticity model for concrete, *Structural Engineering International*, *27(1)*, 68–78, https://doi.org/10.2749/101686616X1081

[13] Lubliner, J., Oliver, J., Oller, S., & Onate, E. (1989) A plastic-damage model for concrete, International Journal of solids and structures, *25(3)*, 299-326, https://doi.org/10.1016/0020-7683(89)90050-4

[14] ACI Committee 363. (1992) Report on high-strength concrete (ACI 363R-92). Farmington Hills, MI: American Concrete Institute.

[15] Dassault Systèmes. (2010) Abaqus/CAE user's manual. Providence, Rhode Island, USA: Abaqus 6.

[16] Labibzadeh, M., Namjoo, H., & Hamidi, R. (2016) Effect of Element Type of Reinforcement on Failure Performance of Four-point Bending beam. *In 4th. International Congress on Civil Engineering, Architecture, and Urban Development*, Shahid Beheshti University, Tehran, Iran.

[17] PCI Committee on Quality Control and Performance Criteria (1983) Fabrication and shipment cracks in prestressed hollow core slab and double tees, *PCI Journal*, *28*(1).

[18] Naser, A. F., Mohammed, H. A., & Mohammed, A. A. (2021). Mathematical modeling of liner static and dynamic analysis for pier height effect on the structural performance of bridge structures, *Journal of Engineering*, *8(4)*, 617–625, https://doi.org/10.18280/mmep.080415

[19] Naser, A. F., Mohammed, H. A., & Mohammed, A. A. (2022) Flexure and shear load rating evaluation of composite bridge superstructure under the effect of different truck load types, *Journal of Engineering*, *57(2)*, 398–407, https://doi.org/10.1016/j.matpr.2021.12.268